PERGAMON

International Journal of Heat and Mass Transfer 44 (2001) 619–632

International Journal of HEAT and MASS TRANSFER

www.elsevier.com/locate/ijhmt

The origin of thermocapillary convection in subcooled nucleate pool boiling

R. Marek[a,*], J. Straub[b]

[a]University of Applied Sciences Deggendorf, Edlmairstrasse 6 + 8, D-94469 Deggendorf, Germany
[b]Karwendelstrasse 10, D-82194 Gröbenzell, Germany

Received 12 January 2000; received in revised form 14 March 2000

Abstract

The significance of noncondensibles as the origin of thermocapillary convection in subcooled pool boiling is demonstrated in this paper. The temperature gradients along the bubble interface inducing thermocapillary convection are caused by saturation pressure gradients due to a nonuniform accumulation of noncondensable gas along the interface. On the vapour side, the noncondensable gas inhibits the condensation of vapour. The corresponding increase of the saturation pressure gradient and temperature gradient, respectively, forces thermocapillary convection on the liquid side of the bubble. A bubble in subcooled liquid can grow or shrink according to the heat and mass transfer at its top, and even a steady-state mass flow through the bubble can be maintained. By a combined analytical and numerical approach the various parameters of this complex system are studied. Furthermore, it is demonstrated that even small amounts of noncondensable gas are sufficient to induce thermocapillary flow. This flow, in turn, inhibits bubble detachment.

Keywords: Boiling; Thermocapillary; Condensation

1. Introduction

By natural and forced convection, only moderate heat fluxes are transferable. For supplying higher amounts of heat in technical equipment at small temperature differences, evaporation and condensation are frequently employed and have gained special importance for reasons of irreversibility and reduction of entropy. Despite intensive research, many questions of boiling and condensation have remained unsolved due to the large number of parameters involved, their interdependence, and the complexity of the corresponding physical mechanisms:

> Boiling is an extremely complex and illusive process, which continues to baffle and challenge inquisitive minds. (V.K. Dhir, 1990 [4])

For practical applications, a variety of empirical heat transfer correlations with a limited range of validity exist. For a long time, gravity was considered the dominant mechanism in nucleate pool boiling. Straub and coworkers [30,34–37,39,40,42–52], as well as Abe et al. [2,26] later on, experimentally proved that the

* Corresponding author. Tel.: +49-991-3615-413; fax: +49-991-3615-499.
E-mail address: rudi.marek@fh-deggendorf.de (R. Marek).

0017-9310/01/$ - see front matter
PII: S0017-9310(00)00124-1

Nomenclature

a	thermal diffusivity (m^2 s^{-1})
F_M	Marangoni force (N)
g	gravitational acceleration (m s^{-2})
h	heat transfer coefficient in the presence of noncondensable gas (W m^{-2} K^{-1})
h_0	heat transfer coefficient in the absence of noncondensable gas (W m^{-2} K^{-1})
Ja_E	Jakob number for evaporation
$\mathscr{K}_{C(E)}$	condensation (evaporation) coefficient
L	characteristic length (m)
$\dot{m}^*_{net}$	specific net mass flow rate (kg s^{-1} m^{-2})
M	mass per mole (kg mol^{-1})
Ma	Marangoni number
Nu	Nusselt number
Nu_0	Nusselt number of pure heat conduction
p	pressure (N/m)
p_c	critical pressure (N m^{-2})
$\mathscr{R}$	universal gas constant (J mol^{-1} K^{-1})
R	bubble radius (m)
T	temperature (K)
x	coordinate (m)
$y_{n,avg}$	average mole fraction of noncondensable gas
$y_{n,i}$	mole fraction of noncondensable gas at the interface
$y_{n,\infty}$	mole fraction of noncondensable gas in the bulk

Greek symbols

ΔT	temperature difference (K)
ΔT_L	subcooling of the liquid (K)
ΔT_W	wall superheat (K)
η	dynamic viscosity (kg s^{-1} m^{-1})
Θ	dimensionless temperature
ξ	dimensionless coordinate
σ	surface tension (N m^{-1})
ψ	contact angle of the bubble (deg)

Subscripts

b	bottom
C	condensation
E	evaporation
l	liquid
n	noncondensable gas
t	top
v	vapour

heat fluxes transferable on earth are also possible in microgravity, especially in subcooled boiling.

Under microgravity, transfer mechanisms other than gravity are dominant, such as bubble coalition, lifting and bubble replacement, mass transport through the bubble, micro wedge evaporation, and thermocapillary convection. Although the phenomenon of thermocapillary convection is known for more than 100 years, it was not paid much attention to due to the dominance of buoyancy flows under earth gravity. Trefethen [41] in 1961 and McGrew et al. [22] in 1966 were the first to point out the importance of surface tension driven convection as gravity-independent heat transfer mechanism in boiling.

In subcooled boiling, thermocapillary flows around vapour bubbles are observed by several authors [43,46,52]. If the top of a growing bubble exceeds the supersaturated boundary layer thus reaching into the subcooled region, the vapour starts to condense [27,29]. With the evaporating liquid, impurities of gas dissolved in the liquid (e.g. air) are gasified at the base of the bubble and carried along with the vapour to the top of the bubble, where the vapour condenses and the noncondensable gas accumulates along the interface. The total pressure of the vapour and the noncondensable gas inside the bubble is determined by the liquid pressure. For a steady-state mass flow through the bubble, the bubble radius remains constant, while the partial pressure of the vapour along the interface and, as a consequence, the saturation temperature decreases towards the top. This gives rise to a temperature gradient along the interface and induces a thermocapillary flow around the bubble directed from the base to the top (cf. Fig. 1). The coupling between this thermocapillary flow and the amount of noncondensable gas is investigated in the following.

2. Thermocapillary or Marangoni convection

2.1. Mechanism of thermocapillary convection

A flow induced by surface tension gradients is termed Marangoni convection after the Italian physicist C.G.M. Marangoni [10–17], or thermocapillary convection if thermal gradients are involved. A review of the history of Marangoni convection and its phenomenology is given in [20]. For most fluids, the temperature gradient of surface tension $\partial\sigma/\partial T$ is negative, i.e. regions of higher temperature exhibit a reduced surface tension. Therefore, thermocapillary convection results in a recirculating fluid flow from the warmer to the colder regions of a liquid (Fig. 1).

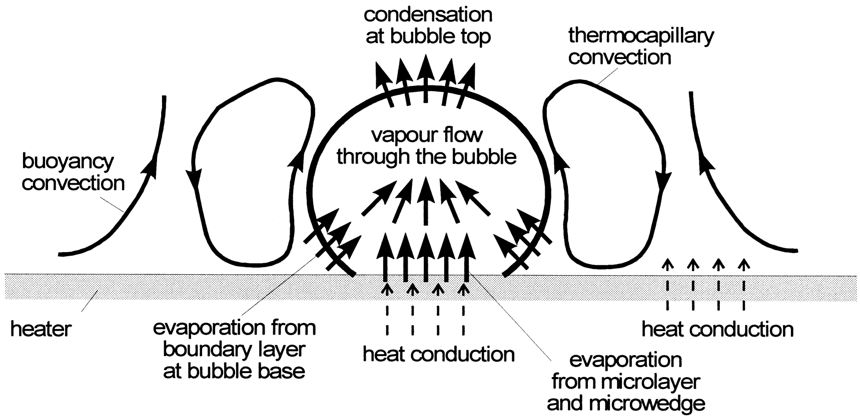

Fig. 1. Heat transfer mechanisms in subcooled boiling.

In saturated pool boiling, the bubble interface is at saturation temperature and shows no temperature gradients, except for the interface in the region of the micro wedge with its high heat flux, which is not considered here. Up to now, no thermocapillary convection could be observed in saturated boiling under microgravity [30,43]. On the contrary, thermocapillary convection is an important heat transfer mechanism in subcooled boiling, as shown under micro and earth gravity conditions by the experiments of Weinzierl [44,46]. Its strength is characterized by the Marangoni number:

$$Ma = \left|\frac{\partial \sigma}{\partial T}\right| \cdot \left|\frac{\partial T}{\partial x}\right| \frac{L^2}{a_l \cdot \eta_l} \tag{1}$$

In several numerical simulations [3,18,19,31–33,38], it could be proved that already small temperature gradients give rise to relatively high fluid velocities along the phase boundary. In order to separate the complex interactions of several mechanisms involved in the boiling process, gas bubbles without phase transition are considered in the first step.

2.2. Marangoni force on bubbles

The thermocapillary flow around a bubble exerts a force on the bubble preventing the bubble from detaching under microgravity and increasing time of bubble attachment under earth gravity. In [20] an analytical model is developed for calculating the reaction force on a gas bubble of spherical shape. The model is applicable both for attached ($\psi > 0$, Fig. 2) and detached bubbles ($\psi = 0$).

For several temperature profiles around the bubble (linear, parabolic, hyperbolic, power law, etc.), analytical solutions for the corresponding Marangoni force were derived and compared to a numerical solution obtained from a two-dimensional flow calculation with finite differences for a detached bubble. Thus, suitable analytical temperature profiles could be determined sufficiently representing the temperature distribution around the bubble within the applied model.

The dimensionless temperature profile Θ around the bubble interface can be expressed by the temperature $T(x)$, the temperatures at the top (T_t) and the bottom (T_b) of the bubble, and a dimensionless coordinate ξ:

$$\Theta(\xi) = \frac{T(x) - T_t}{T_b - T_t} \tag{2}$$

$$\xi = \frac{x}{R} \tag{3}$$

As depicted in Fig. 3, a parabolic temperature profile described by Eq. (4) and a hyperbolic temperature profile described by Eq. (5) were investigated in detail:

$$\Theta_1(\xi) = \frac{1 - 2\xi + \xi^2}{(1 + \cos\psi)^2} \tag{4}$$

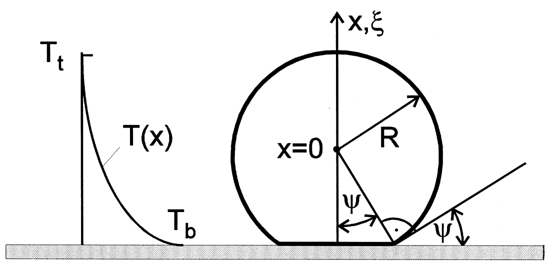

Fig. 2. Bubble in a vertical temperature gradient attached to a heater surface.

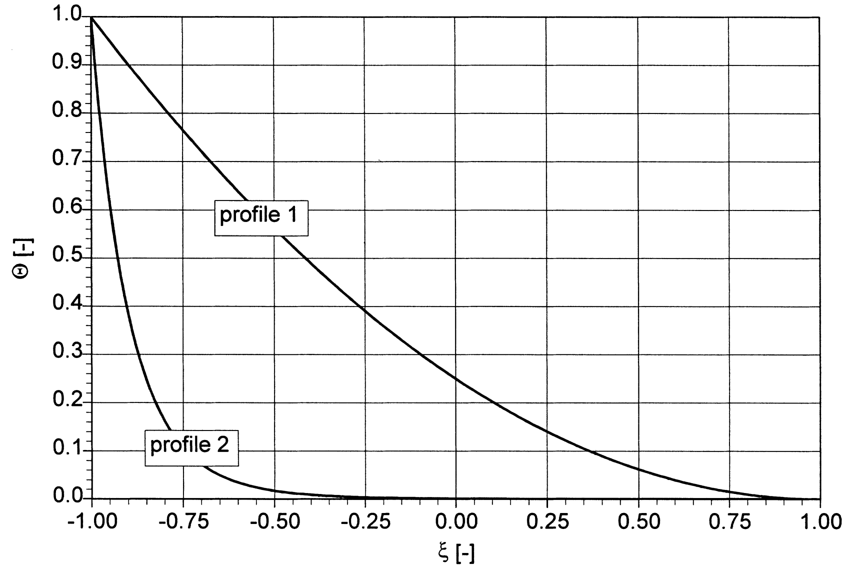

Fig. 3. Investigated dimensionless temperature profiles for a detached bubble ($\psi = 0$).

$$\Theta_2(\xi) = \frac{1}{(2+\cos\psi)^{10}-1}\left[\left(\frac{2+\cos\psi}{\xi+1+\cos\psi}\right)^{10}-1\right] \quad (5)$$

The agreement of the Marangoni force F_M calculated from the parabolic profile with the numerical two-dimensional flow calculation with finite differences is quite good up to $Ma \approx 10^4$ (Fig. 4). For higher Marangoni numbers, the hyperbolic temperature profile yields a better agreement, as the form of the temperature profile is influenced more significantly by the stronger thermocapillary flow.

Another characteristic feature of thermocapillary convection becomes obvious from the numerical calculation. The thermocapillary flow tends to reduce its driving temperature difference. With growing intensity of the thermocapillary convection, i.e. growing Marangoni number, the temperature gradient along the interface is more and more reduced. As shown in Figs. 5

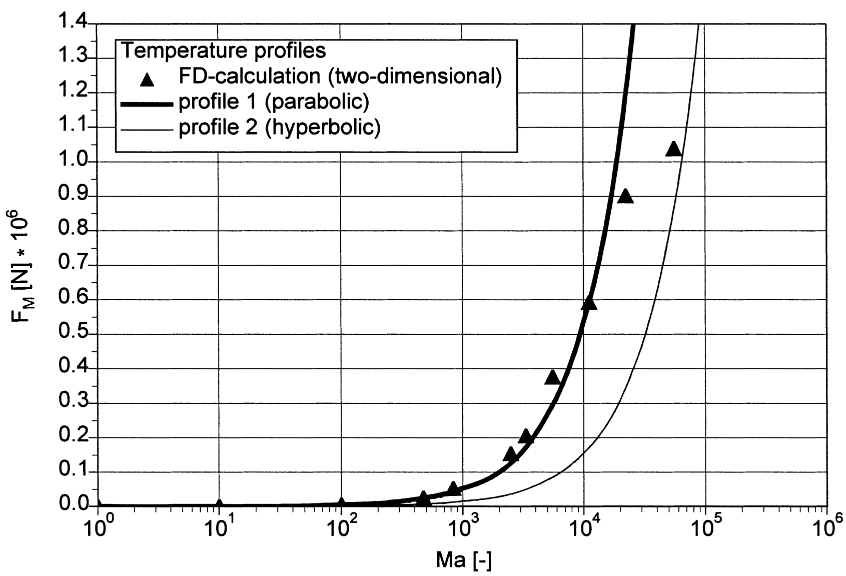

Fig. 4. Comparison of numerically calculated Marangoni force with analytical solutions.

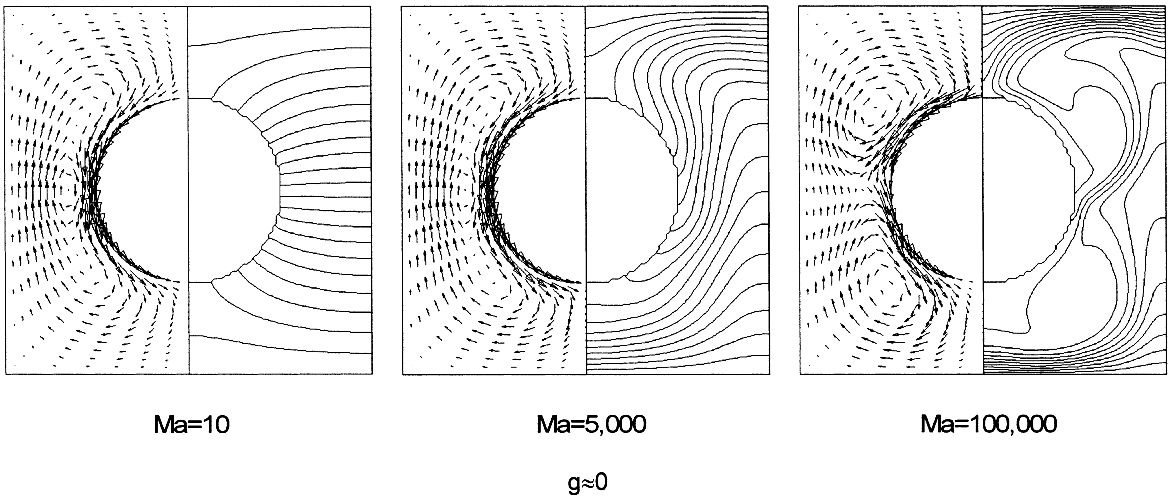

Fig. 5. Flow field (left) and isotherms (right) for a floating bubble under reduced gravity.

and 6, the number of isotherms touching the bubble surface decreases with increasing intensity of the flow.

2.3. Enhancement of heat transfer

In [20,32] the thermocapillary flow around sessile and pending half-spherical bubbles is examined to analyze the influence on the heat transfer. Figs. 7 and 8 show the flow and temperature fields around the bubbles calculated by two-dimensional finite differences. Even for the smallest temperature differences along the bubble interface, i.e. small Marangoni numbers ($Ma = 10$ corresponds to $\Delta T = 1.4 \times 10^{-4}$ K), a fluid motion with a typical toroidal vortex can be observed. In contrast to buoyancy convection, no critical Marangoni number has to be reached for the onset of fluid flow. With growing Marangoni number, the isotherms are displaced from the bubble towards the rigid surfaces leading to an increased heat transfer there.

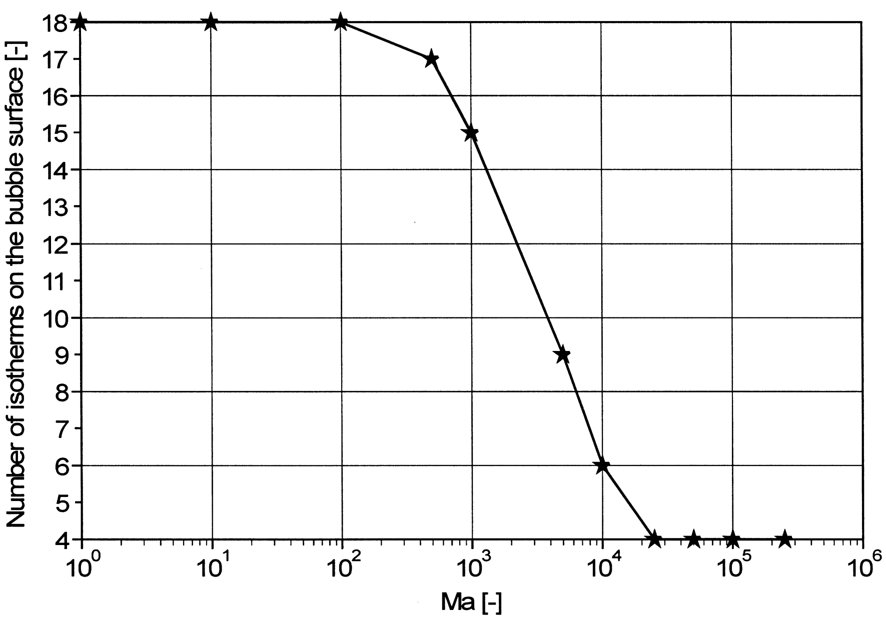

Fig. 6. Decrease of the number of isotherms with increasing Marangoni number.

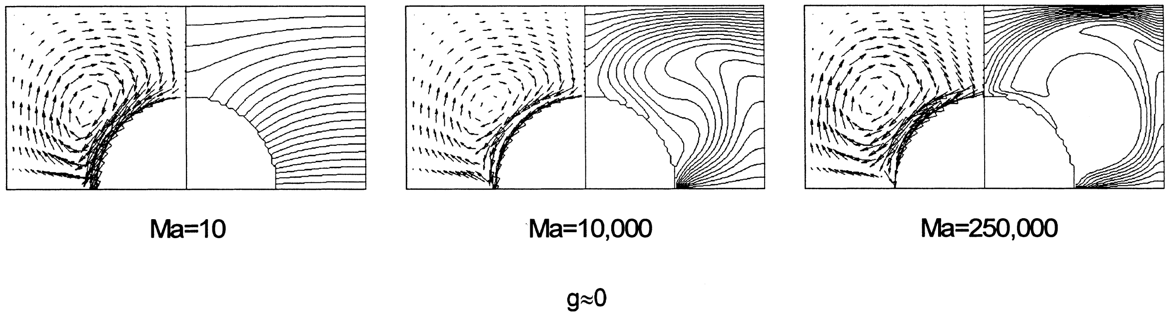

Fig. 7. Flow field (left) and isotherms (right) for a sessile bubble.

The increased heat transfer is depicted in Fig. 9 as the ratio of the Nusselt number with thermocapillary convection Nu and the Nusselt number for pure conduction Nu_0. Experimental confirmation of an enhanced heat transfer by thermocapillary convection is given by Betz [3].

3. Influence of noncondensable gas

3.1. Reduction of heat transfer

Noncondensable gas carried with the vapour towards the interface tends to accumulate there, while the vapour condenses. The gas thus impedes the arrival of new vapour and reduces the heat transfer rate. Fig. 10 shows the reduced heat transfer as the ratio of the heat transfer coefficient in presence of noncondensable gas h and the heat transfer coefficient for pure vapour h_0 for film, direct, and dropwise condensation and different bulk mole fractions of gas $y_{n,\infty}$. Already mole fractions of noncondensable gas of less than 1% reduce the heat transfer significantly.

A theoretical model for calculating the reduced heat transfer in presence of noncondensibles has been developed in [20]. Equalizing the heat flux through the vapour–gas mixture and the heat flux through the condensate, the temperature of the phase boundary can iteratively be calculated. The model has successfully been tested with experimental data for film condensation on a vertical tube [9] (Fig. 11).

3.2. Kinetic evaporation and condensation

Evaporation and condensation across a plane phase boundary are described according to kinetic theory by the Hertz–Knudsen–Schrage equation [8,28]:

$$\dot{m}^*_{\mathrm{net}} = \frac{2}{2-\mathscr{K}_{\mathrm{C}}}\left(\frac{M}{2\pi\mathscr{R}}\right)^{1/2}\left\{\mathscr{K}_{\mathrm{C}}\frac{p_{\mathrm{v}}}{T_{\mathrm{v}}^{1/2}} - \mathscr{K}_{\mathrm{E}}\frac{p_{\mathrm{l}}}{T_{\mathrm{l}}^{1/2}}\right\} \tag{6}$$

For a curved interface, an analogous equation has been deduced [20]

$$\dot{m}^*_{\mathrm{net}} = \frac{4}{4-3\,\mathscr{K}_{\mathrm{C}}}\left(\frac{M}{2\pi\mathscr{R}}\right)^{1/2}\left\{\mathscr{K}_{\mathrm{C}}\frac{p_{\mathrm{v}}}{T_{\mathrm{v}}^{1/2}} - \mathscr{K}_{\mathrm{E}}\frac{p_{\mathrm{l}}}{T_{\mathrm{l}}^{1/2}}\right\} \tag{7}$$

$\mathscr{K}_{\mathrm{E}}$ and $\mathscr{K}_{\mathrm{C}}$ are the evaporation and the condensation coefficient, respectively. An extensive analysis of the

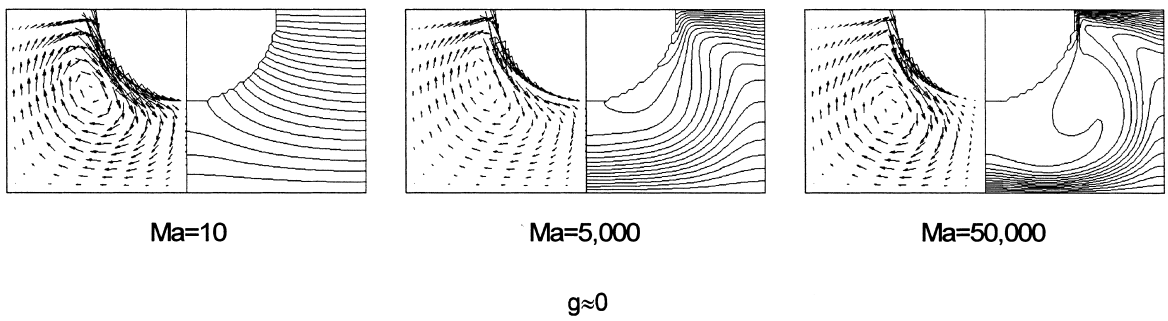

Fig. 8. Flow field (left) and isotherms (right) for a pending bubble.

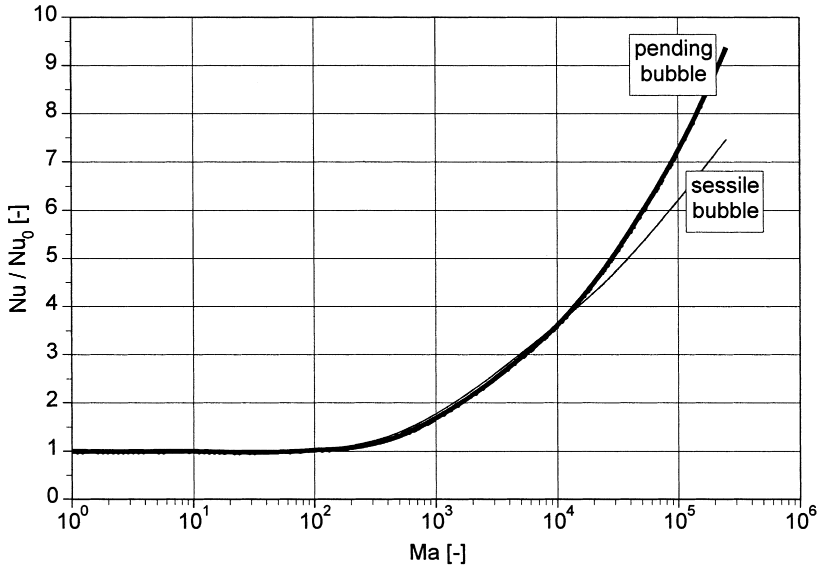

Fig. 9. Relative increase in heat transfer by thermocapillary convection for sessile and pending bubbles.

evaporation and condensation coefficients of water is given in [21]. Frequently, evaporation and condensation coefficients are equalized, although there is no physical justification for this simplification. Eq. (7) is integrated into the numerical model for the accumulation of noncondensibles in bubbles.

3.3. Model for the accumulation of noncondensable gas

In subcooled nucleate boiling, evaporation and condensation are coupled in a very complex manner, as shown in Fig. 12 for an isolated bubble. Due to the superheating of liquid caused by the heat flux from the

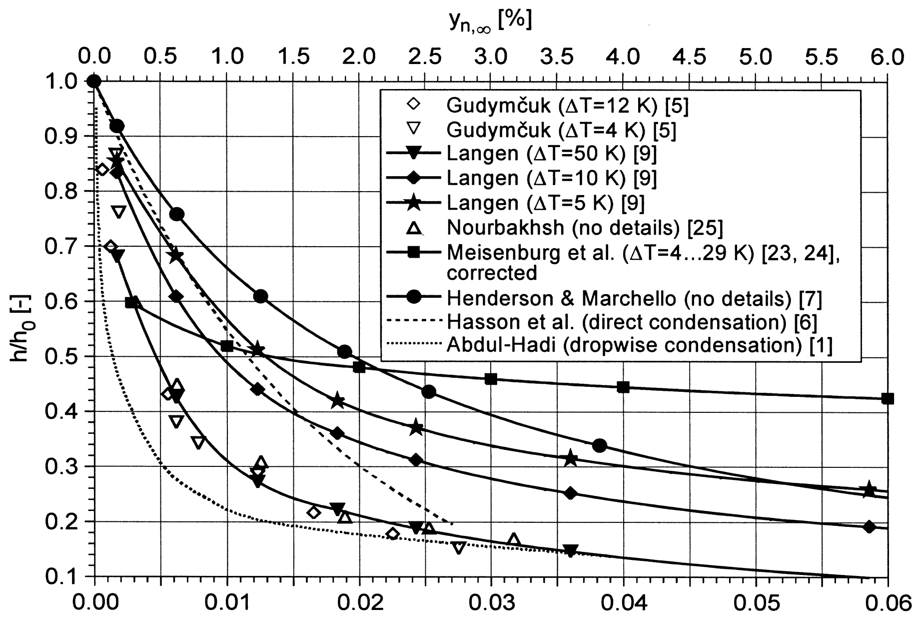

Fig. 10. Reduction of heat transfer in condensation due to noncondensable gas.

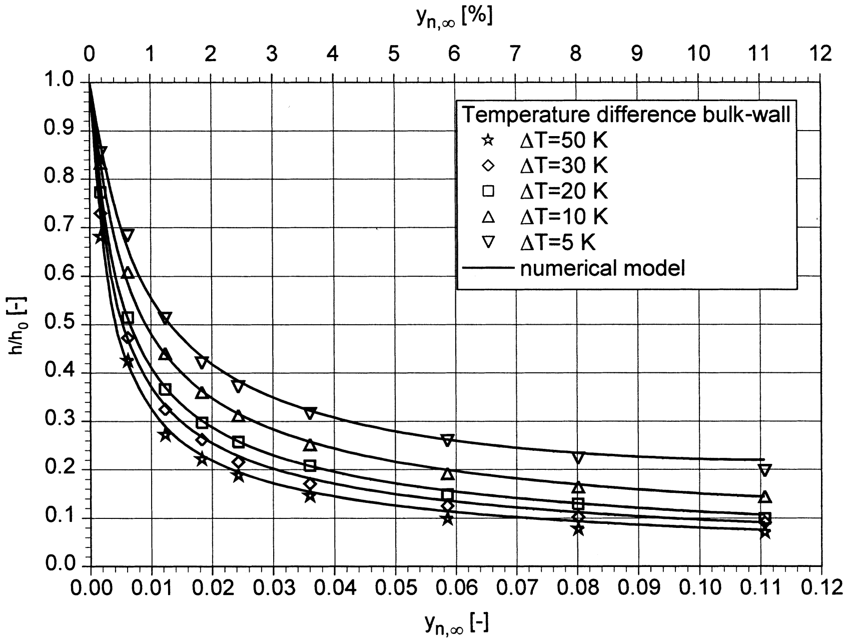

Fig. 11. Comparison of the numerical model (curves) with the experimental data (symbols).

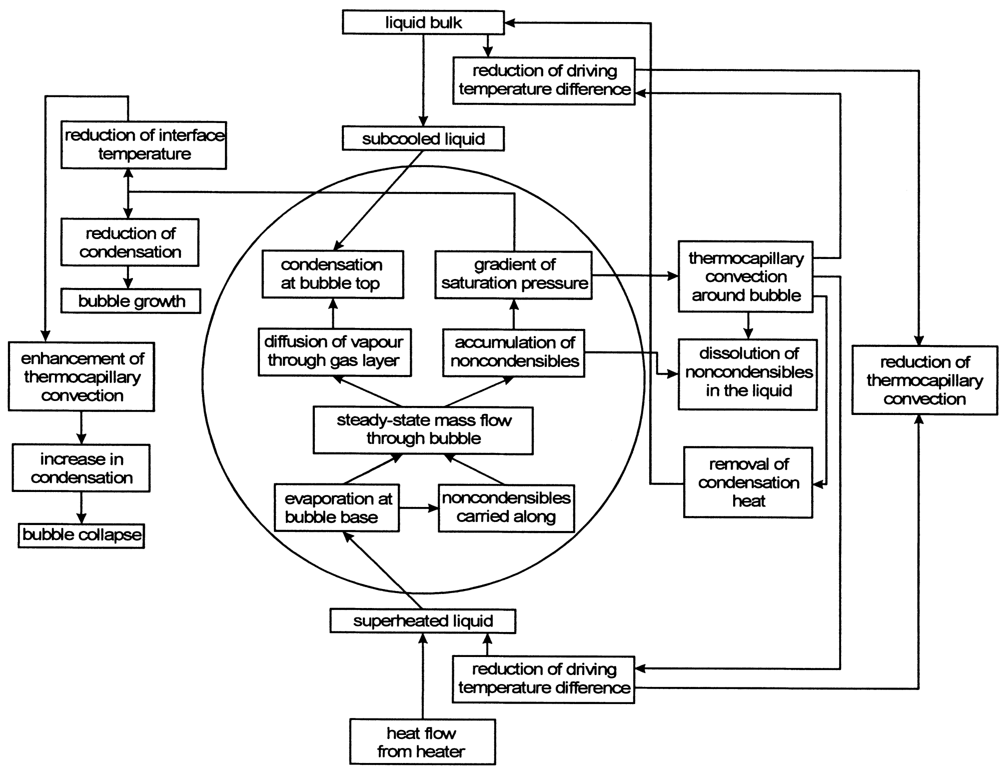

Fig. 12. Interaction of different mechanisms in subcooled boiling for an isolated bubble.

heater at the base of the bubble, vapour evaporates into the bubble and carries along noncondensable gas. Vapour and gas are transported to the top of the bubble, where the vapour condenses due to the subcooling of the surrounding liquid and the noncondensable gas accumulates. The arriving vapour has to diffuse through the stagnant layer of noncondensable gas to condense at the top. Due to the accumulation of gas, the partial pressure of the vapour and the saturation temperature decrease along the interface. The corresponding temperature gradients induce a thermocapillary flow around the bubble, which removes the heat released by condensation of the vapour. The effort of thermocapillary convection to reduce its driving temperature gradient leads to a decrease of the interface temperature near the bubble base and an increase near the bubble top. As a consequence, the intensity of thermocapillary flow around the bubble diminishes. An equilibrium with a steady-state mass transport through the bubble is reached, when the evaporated mass flow rate at the base equals the condensing mass flow rate at the top. The accumulation of noncondensable gas on the top of the bubble increases the concentration difference of the liquid. The accumulated gas partly dissolves into the liquid. This process is favoured by the thermocapillary convection bringing continuously new liquid to the interface.

Gradually the amount of noncondensable gas accumulated at the top of the bubble increases and significantly reduces the interface temperature. According to Eq. (7), this decreases the condensing mass flux. On one hand, a steady-state mass transport through the bubble can no longer be maintained, and the bubble begins to grow. On the other hand, the temperature drop on the vapour side propagates through the interface to the liquid side enhancing the thermocapillary flow around the bubble. As a consequence, the condensation is intensified again due to the increased heat transfer in the liquid, and the bubble begins to shrink. A bubble collapse is limited by a growth process, when the shrinking bubble reaches warmer layers of liquid. Likewise, the growth of the bubble into the subcooled liquid is limited by condensation when the growing bubble reaches colder layers of liquid. Finally, due to these countercurrent effects, a new state of equilibrium is possible for the bubble.

The complete simulation of such a complex system with vapour–gas-flow through the bubble, a moving phase boundary with evaporation and condensation of vapour, accumulation of noncondensable gas in the bubble and dissolution of gas in the liquid, as well as thermocapillary flow around the bubble has not been performed due to limited computer capacities and the aim of the study to clarify basic mechanisms. Therefore, a simplified simulation model focusing on essential processes was developed. As the thermocapillary convection around the bubble has already been studied above, the accumulation of noncondensable gas and the condensation at the top of the bubble, and the influence on the heat transfer is now paid special attention to. The interface of the bubble is treated as spherical and nondeformable. The mass transport model of Robin and Snyder [27,29] is applied for the simulation of a steady-state mass flow through the bubble in combination with Eq. (7). According to Vogel [43], an isolated bubble with a distinct condensation zone and an evaporation zone is considered. The dissolution of noncondensable gas in the liquid is regarded as negligible compared to its accumulation along the interface. The model is summarized in Fig. 13 and described in more detail in [20].

The influence of accumulated noncondensable gas on the condensation at the top of the bubble is quantified followed by the increase in heat transfer (heat transfer coefficient h) necessary to remove the heat of condensation completely for a steady-state mass flow through the bubble. The relative increase in heat transfer is given by h/h_0, where h_0 denotes the heat transfer coefficient in absence of noncondensibles. If this increased heat transfer cannot be provided by the thermocapillary convection around the bubble, the bubble begins to grow, as discussed above. If, on the other hand, the heat transfer by thermocapillary flow is higher than the required amount to remove the heat of condensation, the condensation rate exceeds the evaporation rate at the base, and the bubble shrinks. Thus, the experimentally observed growth and collapse of bubbles with steady-state vapour flow can be explained by the employed model.

3.4. Results

If a certain mole fraction of noncondensable gas in the bulk of the bubble $y_{n,\infty}$ is exceeded, a significant increase in the heat transfer in the liquid is necessary to sustain a steady-state mass transport through the bubble (Fig. 14).

With increasing subcooling, the increase flattens gradually and the bubble is less sensitive to an accumulation of noncondensable gas. However, for small subcoolings, a steep increase in the necessary heat transfer is observed. If the thermocapillary convection cannot provide the necessary heat removal, the bubble grows.

Furthermore, regions, where a steady-state mass flow through the bubble is possible, can be determined from Fig. 14. For a bulk concentration of noncondensable gas of $y_{n,\infty} = 5 \times 10^{-3}$ and a subcooling of $\Delta T_L = 5$ K, no steady-state mass flow is possible due to an infinite necessary heat transfer in the liquid (no intersection of the curve for $\Delta T_L = 5$ K and the line $y_{n,\infty} = 5 \times 10^{-3}$); as a consequence, the bubble grows

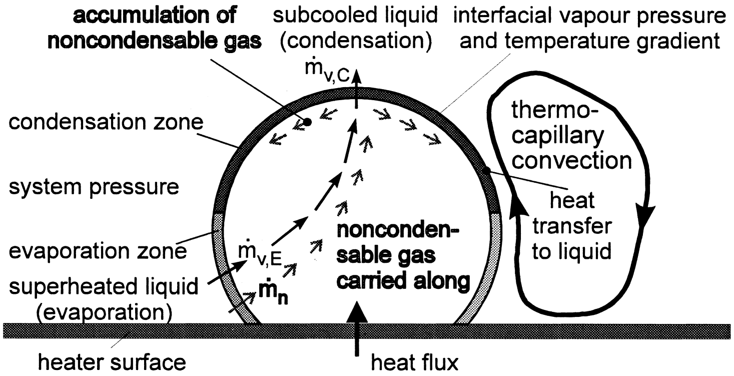

Fig. 13. Nondeformable isolated vapour bubble with steady-state mass flow.

under the given conditions. For $y_{n,\infty} = 5 \times 10^{-4}$, however, a steady-state mass flow through the bubble is possible with a finite increase in heat transfer that can be provided by the thermocapillary convection around the bubble.

The accumulation of noncondensable gas expressed by its mole fraction at the interface $y_{n,i}$ is depicted in Fig. 15 as a function of the concentration of noncondensable gas in the bulk of the bubble $y_{n,\infty}$ and the subcooling of the liquid ΔT_L. As mentioned above, the thermocapillary convection around the bubble cannot provide an arbitrary high removal of heat from the bubble. The corresponding regions of bubble growth are marked with dashed curves in Fig. 15.

The influence of the system pressure on the accumulation of noncondensable gas is depicted in Fig. 16. With rising system pressure, the impediment of condensation at the top of the bubble is displaced towards the lower bulk concentrations of noncondensable gas. Due to the increased system pressure, the mass flows of vapour and noncondensable gas through the bubble are also enhanced. Therefore, higher concentrations of noncondensable gas occur along the interface and the increased heat transfer necessary for a steady-

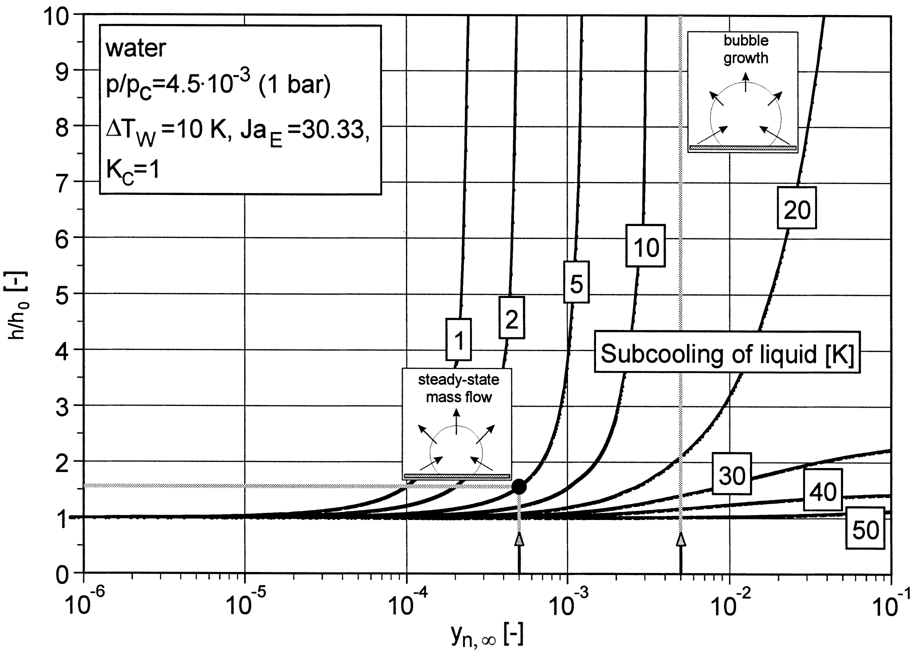

Fig. 14. Increase in heat transfer necessary for steady-state mass flow.

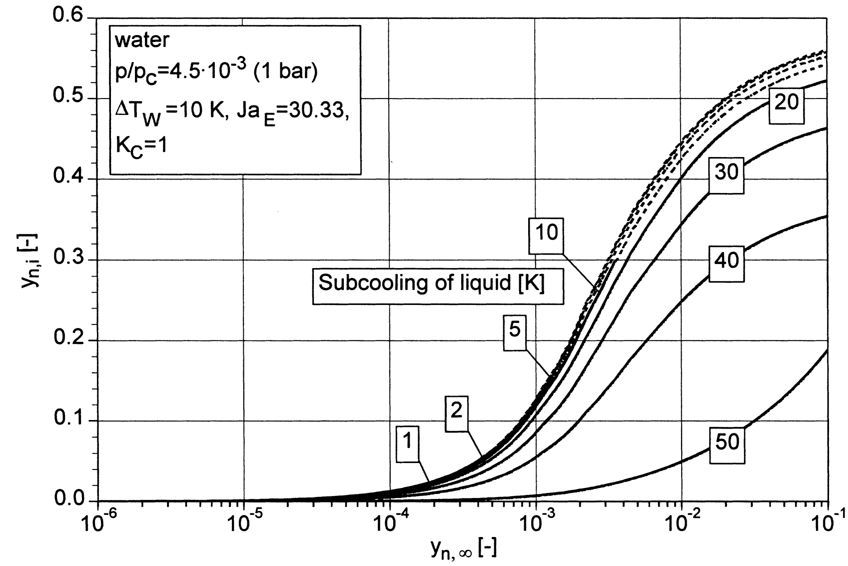

Fig. 15. Mole fraction of noncondensable gas at the interface as a function of bulk mole fraction of noncondensable gas.

state mass flow through the bubble is reached already with lower bulk concentrations of noncondensable gas.

Further results concerning other parameters, such as the wall superheat, the type of fluid, as well as the condensation coefficient, are presented in [20].

The increase of the average concentration of noncondensable gas in the bubble with respect to time is shown in Fig. 17. Depending on the wall superheat ΔT_W, gas concentrations between 2 and 1000 ppm are already reached after 1 ms. Growth times in the order of microseconds for vapour bubbles in saturated boiling on earth are too short for high concentrations of noncondensable gas to build up. However, in subcooled boiling, the bubbles are attached to the heater surface for some milliseconds. Both temperature and partial pressure of the vapour are reduced at the bubble top by the accumulated gas, and thermocapil-

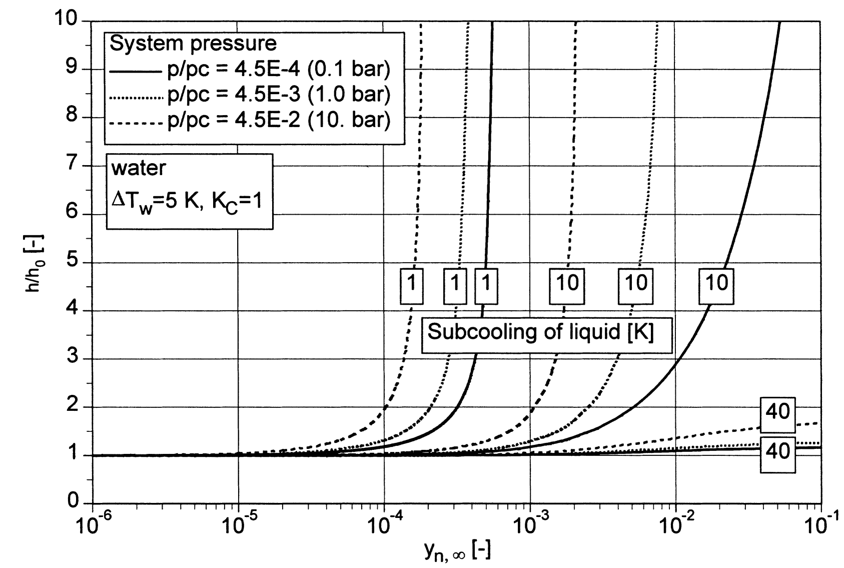

Fig. 16. Increase in heat transfer for different system pressures.

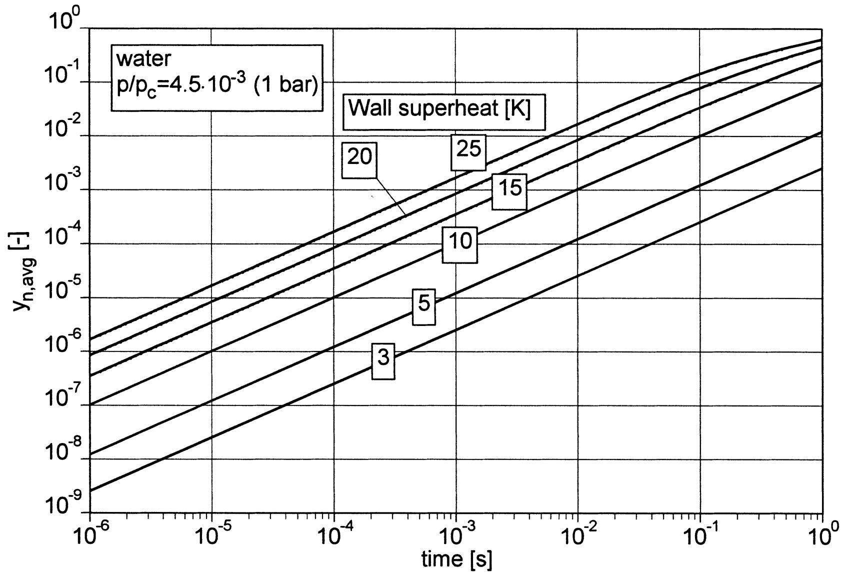

Fig. 17. Increase of the average concentration of noncondensable gas with time.

lary convection around the bubble is enhanced. Especially, under microgravity, where the bubbles do not detach due to the missing buoyancy, high concentrations of noncondensable gas in the bubble are possible.

4. Conclusion

The influence of noncondensable gas as an important source for the thermocapillary flow in subcooled boiling observed in microgravity experiments has been investigated in the previous sections. Due to the complexity and interaction of several mechanisms involved, the individual mechanisms have been de-coupled in simplified models with the aim to clarify basic mechanisms.

The thermocapillary convection around the bubble induced by gradients of saturation pressure and temperature along the bubble surface impedes the detachment of a bubble by a reaction force due to the flow. For small and medium Marangoni numbers, parabolic temperature profiles describe the action of the Marangoni force on the bubble quite adequately. For higher Marangoni numbers, hyperbolic profiles are more suitable, as the form of the temperature profile is directly influenced by the strength of the thermocapillary convection.

To investigate the influence of noncondensable gas on the condensation process in subcooled boiling, an isolated bubble with steady-state mass flow from its bottom to top is considered. Noncondensable gas is carried along with the evaporating vapour at the base of the bubble and accumulates at its top. The diffusion resistance caused by the noncondensable gas impedes the motion of vapour towards the interface. It increases the vapour pressure and temperature gradient along the interface and enhances the thermocapillary flow around the bubble. By the thermocapillary convection, heat is removed from the heater and the bubble, as well.

To ensure a steady-state mass flow through the bubble in presence of accumulated noncondensable gas, an intensified heat transfer in the liquid is necessary, which is possible by the thermocapillary convection. However, the heat transfer rate to remove the heat of condensation cannot be increased arbitrarily. From the performed parameter study, conditions could be revealed, where a steady-state mass flow through the bubble is no longer possible and the bubble begins to grow into the subcooled liquid, which is in accordance with experimental observations.

With increasing subcooling of the liquid or with reduced system pressure, the bubble is less sensitive to the accumulation of noncondensable gas. Transient investigations reveal that within a few milliseconds high concentrations of noncondensable gas can build up in bubbles under steady-state mass flow conditions. Depending on the system parameters, thermocapillary flow can also be observed for bulk mole fractions of noncondensable gas of 10^{-4}. The significance of the accumulation of noncondensable gas for thermocapillary convection is thus emphasized for subcooled nucleate boiling.

Acknowledgements

This work is an excerpt of the thesis of the first author [20] financially supported by the Deutsche Forschungsgemeinschaft (DFG) under grant Str 117/29-2 and subsequently by the Loschge Foundation of the Technical University of Munich, which is gratefully acknowledged.

References

[1] M.I. Abdul-Hadi, Dropwise condensation of different steam–air mixtures on various substrate materials, Can. J. Chem. Eng. 57 (1979) 451–458.
[2] Y. Abe, Pool boiling under microgravity, Microgravity Sci. Technology 6 (4) (1993) 229–238.
[3] J. Betz, Strömung und Wärmeübergang bei thermokapillarer Konvektion an Gasblasen, Ph.D. Thesis, Technical University of Munich, 1997.
[4] V.K. Dhir, Nucleate and transition boiling heat transfer under pool boiling and external flow conditions, in: Proc. 9th Int. Heat Transfer Conf., Jerusalem, Israel, vol. 1, 1990, pp. 129–155.
[5] V.A. Gudymčuk, Teploperedača pri Kondensacii para na naklonnoj trubke (Heat transfer in condensation of steam on an inclined tube), Izvestija Vsesojuznyj Teplotechničeskij Institut 12 (1935) 15–20.
[6] D. Hasson, D. Luss, U. Navon, An experimental study of steam condensation on a laminar water sheet, Int. J. Heat Mass Transfer 7 (1964) 983–1001.
[7] C.L. Henderson, J.M. Marchello, Film condensation in the presence of a noncondensable gas, J. Heat Transfer, Trans. ASME, Ser. C 91 (1969) 447–450.
[8] R.Ya. Kucherov, L.E. Rikenglaz, The problem of measuring the condensation coefficient, Doklady Akademii Nauk SSSR, Phys. Chem. Sect. 133 (1–6) (1960) 735–737.
[9] E. Langen, Der Einfluß des Luftgehaltes auf den Wärmeübergang bei kondensierendem Dampf, Forschung auf d. Geb. d. Ingenieurwes. 2 (10) (1931) 359–369.
[10] C.G.M. Marangoni, Sull' Espansione delle Goccie di un Liquido Galleggiante sulla Superficie di altro Liquido, Pavia, tip. Fusi, 1865.
[11] C.G.M. Marangoni, Sull' espansione delle goccie, sulle superfici liquide (On the spreading of droplets on the surface of a liquid, excerpt of the paper from 1865), II Nuovo Cimento, Ser. 2 3 (1870) 105–120.
[12] C.G.M. Marangoni, Ueber die Ausbreitung der Tropfen einer Flüssigkeit auf der Oberfläche einer anderen, Poggendorff's Annalen d. Physik u. Chemie 143 (7) (1871) 337–354.
[13] C.G.M. Marangoni, Sul principio della viscosità superficiale dei liquidi stabilitio dal Signor J. Plateau (On the principle of surface viscosity of liquids by Mr. J. Plateau), II Nuovo Cimento, Ser. 2 5/6 (1871) 239–273.
[14] C.G.M. Marangoni, P. Stefanelli, Monografia sulle bolle liquide (Monograph on liquid bubbles), II Nuovo Cimento, Ser. 2 7/8 (1872) 301–356.
[15] C.G.M. Marangoni, P. Stefanelli, Monografia delle bolle liquide (Continuazione e Fine) (Monograph on liquid bubbles), II Nuovo Cimento, Ser. 2 9 (1873) 236–256.
[16] C.G.M. Marangoni, Verteidigung der Theorie der Oberflächenelasticität der Flüssigkeiten. Oberflächenplasticität, Beiblätter zu Poggendorff's Annalen d. Physik u. Chemie 3 (12) (1878) 842–846.
[17] C.G.M. Marangoni, Difesa della teoria dell' elasticita superficiale dei liquidi. Plasticita superficiale (Defence of the theory of surface elasticity of liquids. Surface plasticity), Nuovo Cimento, Ser. 3, 3 (1878) 50–68, 97–115, 193–211.
[18] R. Marek, J. Straub, Three-dimensional transient simulation of Marangoni flow in a cylindrical enclosure under various gravity levels, Microgravity Sci. Technology 4 (2) (1991) 153–154 Extended Abstract of the IUTAM Symp. on Microgravity Fluid Mech., Bremen, Germany.
[19] R. Marek, J. Straub, Three-dimensional transient simulation of Marangoni flow in a cylindrical enclosure under various gravity levels, in: Microgravity Fluid Mechanics, IUTAM Symp. on Microgravity Fluid Mech., Bremen, Germany, 1991, 1992, pp. 99–102.
[20] R. Marek, Einfluß thermokapillarer Konvektion und inerter Gase beim Blasensieden in unterkühlter Flüssigkeit, Ph.D. Thesis, Technical University of Munich, 1996.
[21] R. Marek, J. Straub, Analysis of the evaporation coefficient and the condensation coefficient of water, International Journal of Heat and Mass Transfer 44 (2001) 39–53.
[22] J.L. McGrew, F.L. Bamford, T.R. Rehm, Marangoni flow: an additional mechanism in boiling heat transfer, Science 153 (3740) (1966) 1106–1107.
[23] J.W. Meisenburg, R.M. Boarts, W.L. Badger, The influence of small concentrations of air in steam on the steam film coefficient of heat transfer, Trans. AIChE 31 (4) (1935) 622–637.
[24] J.W. Meisenburg, R.M. Boarts, W.L. Badger, The influence of small concentrations of air in steam on the steam film coefficient of heat transfer, Trans. AIChE 32 (1) (1936) 100–104.
[25] H.P. Nourbakhsh, in: Two-Phase Heat Transfer, Handbook of Thermal Design, McGraw-Hill, New York, 1989, pp. 1.75–1.84 (Chap. 5).
[26] T. Oka, Y. Abe, K. Tanaka, Y.H. Mori, A. Nagashima, Observational study of pool boiling under microgravity, JSME Int. J., Ser. II 35 (2) (1992) 280–286.
[27] T.T. Robin Jr., N.W. Snyder, Bubble dynamics in subcooled nucleate boiling based on the mass transfer mechanism, Int. J. Heat Mass Transfer 13 (1970) 305–318.
[28] R.W. Schrage, A Theoretical Study of Interphase Mass Transfer, Columbia University Press, New York, 1953.
[29] N.W. Snyder, T.T. Robin, Jr., Mass-transfer model in subcooled nucleate boiling, ASME Paper 68-HT-51 (1968).
[30] J. Straub, M. Zell, B. Vogel, Pool boiling in a reduced gravity field, in: Proc. 9th Int. Heat Transfer Conf., Jerusalem, Israel, vol. 1, 1990, pp. 91–112.

[31] J. Straub, J. Betz, R. Marek, Convective heat transfer evoked by thermocapillary flows, Energetika 3 (1992) 127–139.

[32] J. Straub, J. Betz, R. Marek, Numerical simulation of Marangoni convection around gas bubbles in a liquid matrix, in: Proc. 8th Europ. Symp. on Materials and Fluid Sci. in Microgravity, Brussels, Belgium, 1992, ESA SP–333, 1992, pp. 257–264.

[33] J. Straub, R. Marek, Transient three-dimensional numerical simulation of Marangoni flow in a liquid column under microgravity, in: Proc. 8th Europ. Symp. on Materials and Fluid Sci. in Microgravity, Brussels, Belgium, 1992, ESA SP–333, 1992, pp. 95–101.

[34] J. Straub, How microgravity supports research in heat transfer, J. Heat Transfer Soc. Jap. 32 (127) (1993) 96–116.

[35] J. Straub, M. Zell, B. Vogel, Boiling heat transfer in microgravity, in: Proc. Int. Symp. on Aerospace and Fluid Sci., Sendai, Japan, 1993, Inst. Fluid Sci., Tohoku University, 1993, pp. 3–29.

[36] J. Straub, M. Zell, B. Vogel, What we learn from boiling under microgravity, Microgravity Sci. Technology 6 (4) (1993) 239–247.

[37] J. Straub, The role of surface tension for two-phase heat and mass transfer in the absence of gravity, Exper. Thermal Fluid Sci. 9 (1994) 253–273.

[38] J. Straub, J. Betz, R. Marek, Enhancement of heat transfer by thermocapillary convection around bubbles — a numerical study, Num. Heat Transfer, Part. A: Applications 25 (1994) 501–518.

[39] J. Straub, J. Winter, G. Picker, M. Zell, Boiling on a miniature heater under microgravity — a simulation for cooling electronic devices, in: Proc. 30th National Heat Transfer Conf., Portland, USA, 1995, ASME HTD, vol. 305-3, 1995, pp. 61–69.

[40] J. Straub, J. Winter, G. Picker, M. Zell, Study of vapor bubble growth in supersaturated liquid, in: Proc. 30th National Heat Transfer Conf., Portland, USA, ASME HTD, vol. 305-3, 1995, pp. 29–37.

[41] L. Trefethen, On the jet propulsion of bubbles in a heated liquid, Tufts University Mechanical Engineering Rep., 61-8-1, 1961.

[42] B. Vogel, J. Straub, Single bubble experiments in pool boiling — results from TEXUS 26, in: Proc. 8th Europ. Symp. on Materials and Fluid Sci. in Microgravity, Brussels, Belgium, April, ESA SP–333, 1992, pp. 879–886.

[43] B. Vogel, Analyse der Energieströme beim Sieden unter Schwerelosigkeit, Ph.D. Thesis, Technical University of Munich, 1994.

[44] A. Weinzierl, J. Straub, Nucleate pool boiling in microgravity environment, in: Proc. 7th Int. Heat Transfer Conf., Munich, Germany, vol. 4, 1982, pp. 21–27.

[45] A. Weinzierl, J. Straub, Wärmeübergang mit Blasenbildung — Ergebnisse des TEXUS-IIIb-Experiments, Zeitschr. f. Flugwissenschaften u. Weltraumforschung 6 (5) (1982) 339–343.

[46] A. Weinzierl, Untersuchung des Wärmeüberganges und seiner Transportmechanismen bei Siedevorgängen unter Mikrogravitation, Ph.D. Thesis, Technical University of Munich, 1984.

[47] A. Weinzierl, M. Zell, J. Straub, Spacelabnutzung — Untersuchung des Wämeübergangs und seiner Transportmechanismen bei Siedevorgängen unter Schwerelosigkeit, BMFT-Report, FB-W 86–021, 1986.

[48] M. Zell, A. Weinzierl, J. Straub, Nucleate pool boiling in subcooled liquid under microgravity — results of TEXUS experimental investigations, in: Proc. 5th Europ. Symp. on Material Sci. under Microgravity Conditions, Schloß Elmau, Germany, ESA SP-222, 1984, pp. 327–333.

[49] M. Zell, J. Straub, Experimentelle Untersuchung des Wärmeübergangs und seiner Transportmechanismen unter reduzierter Schwerkraft, Jahrbuch d. Technischen Universität München, 1985, pp. 163–178.

[50] M. Zell, J. Straub, Microgravity pool boiling — TEXUS and parabolic flight experiments, in: Proc. 6th Europ. Symp. on Material Sci. under Microgravity Conditions, Bordeaux, France, 1986, ESA SP–256, 1987, pp. 155–160.

[51] M. Zell, J. Straub, B. Vogel, Pool boiling under microgravity, J. Physico-Chem. Hydrodynamics 11 (5/6) (1989) 813–823.

[52] M. Zell, Untersuchung des Siedevorgangs unter reduzierter Schwerkraft, Ph.D. Thesis, Technical University Munich, 1991.